

Impact of brown coal dust on the organic matter in particle-size fractions of a Mollisol

MICHAEL W. I. SCHMIDT¹, HEIKE KNICKER^{1,2}, PATRICK G. HATCHER² and INGRID KÖGEL-KNABNER¹

¹Department of Soil Science, Technical University of Munich, D-85350, Freising-Weihenstephan, Germany and ²Energy and Fuels Research Center, 209 Academic Projects Building, The Pennsylvania State University, University Park, PA 16802, U.S.A.

Abstract—The influence of brown coal emissions from a briquette factory on the organic matter of a Mollisol has been investigated. Non-contaminated, heavily contaminated soils and airborne particles are compared by using chemical and spectroscopic methods (¹³C CPMAS-NMR, Py-GC-MS, ¹⁴C dating). Bulk soils as well as their particle-size fractions are investigated. Organic carbon content of the bulk contaminated soil (138.6 g C/kg) is higher by a factor of six than the non-contaminated soil. For particle-size fractions, the highest content of organic carbon is found in the fine sand fraction (347.2 g C/kg). Furthermore, organic matter of the contaminated site shows a trend for relatively higher abundance of aliphatic compounds in the fraction ranging from 6 to 2000 μm, whereas for particles < 6 μm no trend was observed. The A horizon of the contaminated soil is much older (15,750 yr BP) than the non-contaminated soil, which indicates input of anthropogenic material. Py-GC-MS analyses show for the non-contaminated site a homologous series of mainly alkanes, low amounts of prist-1-ene and a high abundance of lignin- and carbohydrate-derived structures. In contrast, composition of the samples from the contaminated site are similar to a sample of brown coal analyzed and show a homologous series of *n*-alkane, alkene, α , ω -alkadiene triplets and a high relative abundance of prist-1-ene with few lignin derived compounds, except for the clay fraction. Reflected light microscopy shows large amounts of brown coal dust particles with typical maceral groups, huminite, liptinite, and inertinite, in the fine sand fraction from the contaminated soil. Additionally, minor amounts of thermally altered brown coal-derived particles, i.e. coke particles, are observed. Copyright © 1996 Elsevier Science Ltd

Key words—brown coal dust, soils, Mollisol, size fractions, ¹³C CPMAS-NMR, Py-GC-MS, ¹⁴C dating

INTRODUCTION

Coal has been used for centuries as an energy supply, basically for combustion purposes. As a consequence, emissions, soot, other coal-like particles and airborne dust have been released in tremendous amounts, ubiquitously dispersed and supposedly accumulated in the environment. For the East German industrial region around Bitterfeld, atmospheric deposition of dust, mainly from the brown coal processing industry, resulted in accumulation of 0.7 m (average thickness) over an area of 850 km² during the last 100 yr (Neumeister *et al.*, 1991). Previous studies showed that the pollution of the environment may be associated with coal utilization. Coal, soot and char particles have been identified, for instance, in an Australian lake (Depers and Yassini, 1994) as well as in remote Swedish forest soils (Wik and Renberg, 1987).

There are only a few investigations on the stability of soot and coal in soils. For bituminous coal, both natural *in situ* oxidation (Fredericks *et al.*, 1983) and laboratory oxidation (Pisupati *et al.*, 1993) were studied. Investigating the microbial degradation of soot in natural soils, Shneour (1966)

found that after 3 months only 2% of the added soot was mineralized. Due to constant replenishment and low decomposition rates, it can be assumed that airborne soot and coal-like particles will accumulate in soils, especially in heavily industrialized areas where these emissions can supposedly contribute significantly to the organic matter content of the soils.

The impact that lignite, bituminous or anthracite coal or other coal-like emissions have on the chemical properties (e.g. sorption of hydrophobic organic compounds in soils) is poorly understood (Schmidt and Kögel-Knabner, 1995). Lignite, bituminous or anthracite coal and brown coal laden wastewater and sediment can act as sorbents for hydrophobic organic compounds (Garbarini and Lion, 1986; Grathwohl, 1990; Kopinke *et al.*, 1995).

The objective of this study was to compare the structural characteristics of the soil organic matter at a site highly contaminated with airborne coal and/or coal combustion-derived emissions with a corresponding non-contaminated soil. The impact of brown coal emissions on both quantity and quality of the natural organic material in the bulk soil and its particle-size fractions was determined. The

particle-size fractions and the bulk soils were investigated by a combination of spectroscopic methods (solid-state ^{13}C NMR spectroscopy, pyrolysis–gas chromatography–mass spectrometry, carbon isotopic composition) and analysis of ^{14}C as well as classical bulk methods (elemental analysis, reflectance microscopy).

MATERIAL AND METHODS

Sample description

The study area is situated in the highly industrialized region of Halle (Germany), which has been dependent on the industrial use of brown coal for more than 100 yr. The two sites investigated have been farmland since the beginning of this century. For the contaminated site south of Halle, close to Beuna, the source of pollution was mainly emissions from a factory which combusted brown coal to obtain energy and produce briquettes. The sampling site is situated about 1 km downwind of the factory. Because factory emissions are expected to be the major pollutants, a brown coal sample of the last production series was taken for comparison purposes. A non-contaminated soil north of Halle, Gut Seeben was also sampled. Both soils were classified as Udorthentic Haplustoll (Soil Survey Staff, 1994).

Sample pretreatment and particle-size separation

Roots and visible plant remains were mechanically removed from the samples whenever possible. The samples were frozen (-30°C) and later freeze-dried at a temperature of -60°C and an air pressure of 8 Pa (Edwards Freeze Dryer, Super Modulayo). Soil aggregates were carefully crushed and the fraction >2 mm was removed by dry sieving. For chemical bulk analysis an aliquot was ground in a ball mill for 10 min. Particle-size fractionation of the plow (Ap) horizons was performed by a combination of wet sieving and sedimentation following dispersion with ultrasonic treatment (Christensen, 1985, 1992). The ultrasonic energy was applied with an ultrasonic probe (Labsonic U, Braun Melsungen, FRG) using a 19 mm diameter titanium probe. The energy applied was 440 J/ml (North, 1976). The temperature of the suspension (30 g soil/150 ml water) was kept below 35°C . By wet sieving, the suspension was separated into three sand fractions (630–2000 μm , 200–630 μm , 63–200 μm). The clay fraction (<2 μm) and three silt fractions (20–63 μm , 6–20 μm , 2–6 μm) were obtained by sedimentation in graduated cylinders. The fractions were recovered from the suspensions by filtration with pre-washed cellulose nitrate filters (0.45 μm). The filter pellets could be easily removed from the filter and were freeze-dried, weighed, and milled.

Elemental analyses

Carbon and nitrogen contents of the bulk soils and the various fractions were determined in duplicate for the non-contaminated site with a Leco CNS 2000 and for the contaminated site with an Elementar Vario EL. The content of dissolved organic carbon in suspension was determined with a Shimadzu TOC Analyzer.

Solid-state ^{13}C NMR spectroscopy

Solid-state ^{13}C NMR spectra were obtained on a Bruker MSL 100 and a Chemagnetics 100 (both 2.35 T) using the technique of cross polarization and magic angle spinning (CPMAS). The parameters were as follows: contact time 1.0 ms; pulse delay 100–600 ms, 50 kHz of proton decoupling; sweep width of 10 kHz and 0.5 K of data zero-filled to 4 K (Zhang *et al.*, 1993). For each spectrum 20–600 $\times 10^3$ scans were obtained. Samples low in organic carbon (all bulk samples and size fractions from the non-contaminated site and the bulk sample from the BvCv horizon of the contaminated site) were treated three times with HF (10%), washed three times with distilled water, filtered (0.45 μm) and freeze-dried. Chemical alterations due to HF treatment are expected to be minimal (Skjemstad *et al.*, 1994).

Py–GC–MS

Pyrolysis–gas chromatography–mass spectrometry (Py–GC–MS) was performed with a Chemical Data System Pyroprobe 1000. Between 0.5 and 14 mg of sample was heated in a quartz tube at a rate of $5^\circ\text{C}/\text{ms}$ for 10 s to a final temperature of 610°C . The pyroprobe was secured in the injection port of the gas chromatograph. Pyrolyzates were cryofocused onto the GC column with liquid nitrogen and then chromatographed in a Varian 2700 gas chromatograph with injection port at 280°C equipped with a J and W DB 17 capillary column (30 m \times 0.25 mm). Mass spectra were obtained on a Dupont 21-490B mass spectrometer directly coupled to the gas chromatograph and processed with a Teknivent Vector/One data system interfaced to the mass spectrometer. Structure assignments for the various peaks were based on literature reported mass spectra and NBS/Wiley library mass spectra.

Radiocarbon dating

Carbon was extracted from the samples by combustion and transferred to benzene; then the ^{14}C activity was measured by liquid scintillation counting (Becker-Heidmann *et al.*, 1988). Part of the sample was combusted, the CO_2 was purified and its $\delta^{13}\text{C}$ determined in an isotope mass spectrometer. Further details of sample preparation and measurement procedure of radiocarbon and stable isotopes are given by Becker-Heidmann (1989). The radio-

carbon dates were corrected for isotopic fractionation according to Stuiver and Polach (1977).

Reflected light microscopy

Samples for microscopic analysis were prepared by first making a cylindrical mold of polyester resin (Epolite 53/3 epoxy resin, Hexcel, Chatsworth CA) leaving a cavity (5 mm × 15 mm × 25 mm) on the center top. The sample was mixed with the resin within the cavity and allowed to set. The surface was then polished and examined microscopically in reflected light within oil immersion using a Zeiss Axiophot microscope.

RESULTS AND DISCUSSION

C and N content of bulk samples

The characteristic feature of Mollisols is a deep, dark-colored surface (A) horizon. In the A horizon of Central European Mollisols the content of or-

ganic C varies between 20 and 60 g/kg with a narrow C/N ratio of about 10. The non-contaminated soil contains 22.6 g C/kg air dry soil and 2.0 g N/kg air dry soil in the Ap horizon (Table 1). These values are within the range expected for this soil type (Dalal and Bridge, 1996). The contaminated site shows values which are six times higher for C and twice for N compared with the non-contaminated site. The non-contaminated soil shows typically low C/N ratios (around 11) for all three horizons. In contrast, the C/N ratios of the contaminated soil are high (around 40) in the plowed horizons (Ap1 and Ap2) and decrease to values similar to the non-contaminated site in the BvCv horizon. The extremely high contents of organic carbon in the A horizons together with the high C/N ratios indicate the input of a C-rich and N-poor material in the topsoil. For instance, the brown coal sampled in the briquette factory is very rich in C (554.4 g C/kg) and relatively low in N (C/N ratio

Table 1. Soil description*, mass distribution, content and distribution of C and N in the non-contaminated and contaminated soil for bulk soils and particle-size fractions

Soil/sample	% of total mass	g/kg [†]	Total OC % of total OC	g/kg, [†]	Total N % of total N	C/N
Non-contaminated bulk soil						
<i>sampling depth (cm)</i>						
Ap	100.0	22.6	100.0	2.0	100.0	11
Ah	100.0	21.0	100.0	1.9	100.0	11
ICAh	100.0	12.9	100.0	1.3	100.0	10
<i>particle size (µm)</i>						
coarse sand	1.7	10.8	0.9	0.2	0.2	54
medium sand	10.1	2.7	1.2	0.1	0.4	44
fine sand	15.9	6.5	4.9	0.2	1.8	39
coarse silt	28.3	3.2	4.3	0.1	2.0	29
medium silt	12.4	19.2	11.2	1.0	8.1	19
fine silt	5.8	62.9	17.2	4.1	15.2	16
clay	20.2	62.9	59.9	5.7	75.2	11
DOM [‡]	—	—	1.0	—	—	—
% recovery	94.4	—	100.6	—	102.9	—
Contaminated bulk soil						
<i>sampling depth (cm)</i>						
Ap1	100.0	138.6	100.0	3.6	100.0	39
Ap2	100.0	140.6	100.0	3.5	100.0	40
BvCv	100.0	12.4	100.0	1.1	100.0	11
Cv	100.0	<0.1	100.0	<0.3	100.0	—
<i>particle size (µm)</i>						
coarse sand	0.5	29.5	0.1	1.7	0.3	17
medium sand	1.8	52.5	0.8	1.5	0.9	35
fine sand	12.7	347.2	36.1	5.2	21.4	67
coarse silt	30.9	58.4	14.7	1.0	10.0	58
medium silt	17.0	159.2	22.1	3.1	17.0	51
fine silt	8.0	198.5	12.9	6.0	15.4	33
clay	17.6	126.4	18.2	6.8	38.7	19
DOM [‡]	—	—	0.7	—	—	—
% recovery	88.5	—	105.6	—	103.7	—
Brown coal	100.0	554.4	100.0	6.3	100.0	88

*Horizon designations are according to AG Bodenkunde (1994).

[†]Content is expressed as g/kg bulk soil or size fraction.

[‡]Dissolved organic matter: after filtration the content of dissolved organic carbon was determined for the fraction <0.45 µm with an aliquot of the solution and from this data % of total organic C was calculated.

— not determined.

88) and could therefore be responsible for the observed distribution of C and N at the contaminated site.

C and N contents and distribution for particle-size fractions

Table 1 gives the results obtained from particle-size fractionation of the topsoil samples (Ap and Ap1 horizons). The non-contaminated site shows a clear pattern both for content and distribution of C and N. The content of C and N is highest in the fine silt and clay fraction. The clay fraction contributes approximately 60% of the total carbon and 75% of the total nitrogen to this Ap horizon. The C/N ratios decrease systematically from the sand to the clay fractions. As similar data have been reported for Mollisols and other soils (Baldock *et al.*, 1992; Christensen, 1992; Guggenberger *et al.*, 1995) we can assume that this is a typical pattern for non-contaminated soils.

On the other hand, a completely different pattern is found for C and N contents of the contaminated soil (Table 1). The content of C is highest in the fine sand fraction (347.2 g/kg) whereas the N is highest in the clay fraction (6.8 g/kg). The contents of C are between 2 (clay) and 53 (fine sand) times higher than in the non-contaminated soil. Contrasting with the non-contaminated site, the clay fraction of the contaminated soil contributes with only 18% of the total carbon and 39% of the

total nitrogen to this horizon. C/N ratios of the size fractions show a different distribution compared to those in the non-contaminated soil. The mid-range size particles (fine sand, coarse and medium silt fraction) show extremely high C/N ratios, which indicate an input of material rich in C and/or poor in N. Mineral airborne particles with an average density of 2.6 Mg/m³ transported over longer distances are usually in the range of clay and fine silt size (Simonson, 1995), whereas the C-rich particles from the contaminated site are found in coarser fractions (medium silt to fine sand). Therefore we can expect these particles to be transported over a shorter distance, or to have a lower density, or both.

¹³C CPMAS-NMR spectroscopy

The ¹³C CPMAS-NMR spectroscopic investigation of the bulk soils (Fig. 1) shows rather similar spectra for all horizons of the non-contaminated site (Fig. 1a–c). Only the spectrum of the plowed topsoil (Fig. 1a) shows a slightly higher intensity in the region of carbohydrates (45–110 ppm), most probably due to the input of plant litter. Similar spectra are reported for other Mollisols (e.g. Baldock *et al.*, 1992). Contrasting, the contaminated site shows similar, almost identical spectra for the two plowed top horizons (Fig. 1d, e) and a different pattern for the BvCv horizon (Fig. 1f), which is more similar to the spectra of the non-contaminated site. The spectra of the plowed top horizons of the

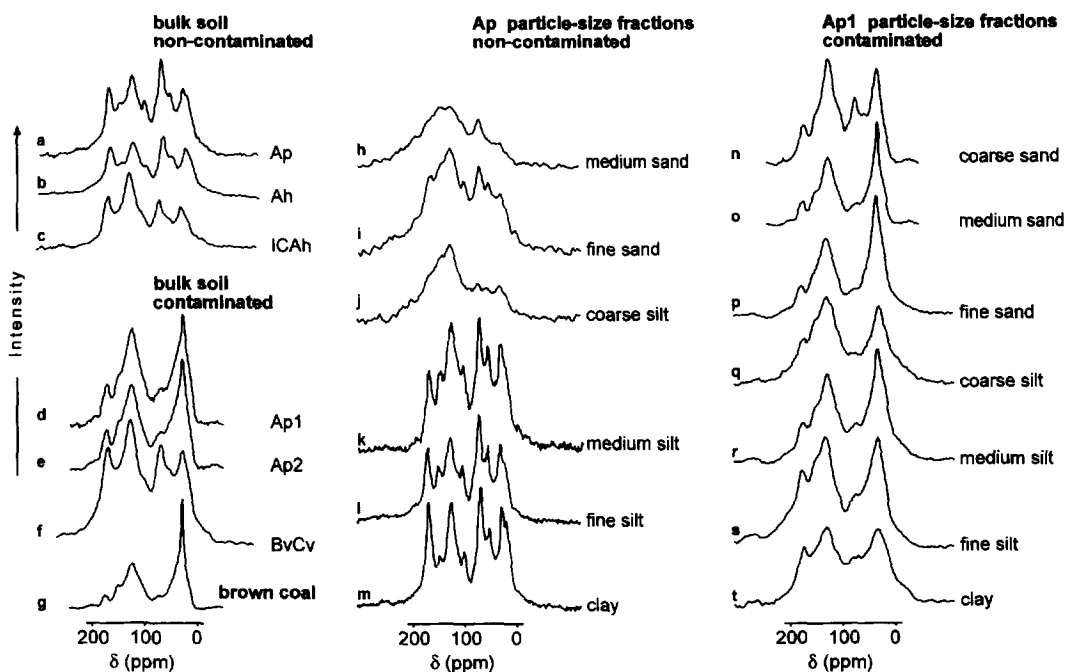


Fig. 1. ¹³C CPMAS-NMR spectra of brown coal, bulk horizons and particle-size fractions from the contaminated and non-contaminated soil. The particle-size fractions are clay (< 2 μm), fine silt (2–6 μm), medium silt (6–20 μm), coarse silt (20–63 μm), fine sand (63–200 μm), medium sand (200–630 μm) and coarse sand (630–2000 μm).

contaminated site are dominated by signals in the alkyl C (0–45 ppm) and aromatic C (110–160 ppm) region. The brown coal sample (Fig. 1g) shows a similar spectrum with more distinct peaks for alkyl and aromatic C, a phenomenon which has been reported for many brown coals (Wilson, 1987; Meiler and Meusinger, 1991).

Considering the similarity between the brown coal and top sections of the contaminated site we considered the distinct dominance of alkyl and aromatic C as a fingerprint for brown coal and calculated a ratio for the signal intensities, called A:

$$A = [\text{alkyl C} + \text{aromatic C}] / [\text{O-alkyl C} + \text{carboxylic C}] \quad (1)$$

Table 2 contains the calculated ratios of the samples analyzed. Brown coal has an A of 2.3. The

non-contaminated site shows lower A both for the top horizons (A = 0.9) and the subsoil (A = 1.2). Data for other Mollisols from Baldock *et al.* (1992) yielded similar values for A. The contaminated site shows higher A both for Ap1 (A = 1.8) and Ap2 (A = 1.6) horizons, whereas the value of A for the subsoil is lower (A = 1.0) and similar to the non-contaminated site. This can be taken as another indication of the influence of brown coal-like contamination which was incorporated into the soil by plowing.

The NMR spectra of the size fractions are shown in Fig. 1h–t. For the size fractions the calculated A also indicates evidence of the contribution of brown coal (Table 2). The ratios A in the size fractions of the non-contaminated site range from 0.8 to 1.1. A values for particle-size fractions of another Mollisol

Table 2. Relative areas* of peaks in ^{13}C CPMAS-NMR spectra of bulk soils and particle-size fractions from non-contaminated and contaminated soils in comparison with the brown coal sampled in the briquette factory Beuna

	Alkyl C %	O-alkyl C %	Aromatic C %	Carboxyl C %	Alkyl + aromatic/ O-alkyl + carboxyl C (A) [†]	Anthropogenic organic C [‡] (% of total OC)
Non-contaminated						
<i>bulk soil</i>						
Ap	20	35	28	16	0.9	
Ah	21	32	27	20	0.9	
ICAh	18	29	36	17	1.2	
<i>Ap / size fractions</i>						
coarse sand	—	—	—	—	—	
medium sand	8	29	36	27	0.8	
fine sand	13	32	35	20	0.9	
coarse silt	13	26	39	22	1.1	
medium silt	20	34	32	14	1.1	
fine silt	22	39	29	10	1.0	
clay	25	36	27	12	1.1	
Contaminated						
<i>bulk soil</i>						
Ap 1	28	26	36	10	1.8	
Ap 2	27	27	34	11	1.6	
BvCv	19	30	31	20	1.0	
<i>Ap / size fractions</i>						
coarse sand	23	32	36	10	1.4	
medium sand	32	24	36	9	2.1	
fine sand	37	22	31	10	2.1	
coarse silt	28	23	33	16	1.6	
medium silt	37	23	31	9	2.1	
fine silt	25	23	32	20	1.3	
clay	29	27	28	16	1.3	
Contamination[‡]						
bulk soil Ap1	25	21	27	7	2.0	80
coarse sand	—	—	—	—	—	—
medium sand	32	23	34	8	2.2	97
fine sand	36	21	30	10	2.1	97
coarse silt	27	22	31	15	1.6	95
medium silt	35	19	27	8	2.4	89
fine silt	18	11	23	17	1.5	69
clay	17	10	14	10	1.6	51
brown coal	36	23	34	7	2.3	

*Data in % of total signal intensity (alkyl C –10 to 45 ppm, O-alkyl C 45 to 110 ppm, aromatic C 110 to 160 ppm, carboxyl C 160 to 220 ppm).

[†]As defined in equation 1.

[‡]Assuming both soils originally contained the same amount and distribution of organic C and no further alterations occurred, the amount of anthropogenic organic carbon (C_{cont}) was calculated by equation (2) and expressed as (i) % of total organic C in the fraction (data from Table 1) and (ii) for the different types of C in the respective chemical-shift region.

— not determined.

were calculated from data reported by Baldock *et al.* (1992). The calculated A values for particle-size fractions between 2000 to 0.2 μm vary between 0.5 and 0.9 and are similar to those obtained in this study for the non-contaminated soil. The fractions from the contaminated site show higher A values. Increased A (1.6–2.1) of the particles within the medium sand to medium silt fractions (630–6 μm) are similar to the A value of brown coal. Finer fractions present lower A values, which are more similar to those found in the non-contaminated fractions.

The contaminant contribution to soil organic matter content and composition can be estimated by the following calculations. One can calculate the content of organic carbon originating from brown coal contamination (C_{cont}) in bulk soil and size fractions, assuming both soils originally contained the same content of organic carbon, by

$$C_{\text{cont}} (\text{g/kg}) = [\text{OC} (\text{g/kg}) \text{ contaminated}] - [\text{OC} (\text{g/kg}) \text{ non - contaminated}]. \quad (2)$$

The relative contribution of C_{cont} to the bulk soil and the individual particle-size fractions is given in Table 2. The contribution of C_{cont} decreases continuously from medium sand (97%) towards finer fractions (clay: 51%). This suggests that mainly the coarser particle-size fractions are affected by the emissions. Together with the ^{13}C NMR data one can also calculate the content of emission-derived organic carbon (C_{cont}) for each type of C in the respective chemical-shift region, again assuming the nature of soil organic matter was identical in both soils prior to contamination. The data then represent the calculated composition of the contaminant in the four chemical-shift regions of the NMR spectra, given as percentage values similar to the ^{13}C NMR integrals obtained by spectroscopic analysis (Table 2). The high A values calculated for C_{cont} clearly indicate the fingerprint of brown coal not only for the bulk soil ($A = 2.0$) but also for the size fractions ($A = 1.5\text{--}2.4$).

Differences in the quality of soil organic matter as revealed by ^{13}C CPMAS-NMR spectroscopic investigation could be taken as an indication that brown coal emissions have been accumulating in the soil for decades without major degradation. The NMR spectra of the fractions have a brown coal fingerprint with the distinct peaks in the aromatic and aliphatic region. The impact of brown coal dust is more pronounced in the coarse particle-size classes than in the fine particle-size classes.

^{14}C dating

Considering the elevated age of brown coals, compared with soils, in case of contamination a much higher ^{14}C age in the contaminated than in the natural soil should be expected, as a consequence of contamination by older material. The

brown coal sample, most probably of Tertiary origin, cannot be dated, because it is beyond the time covered by ^{14}C determination and contains only so-called dead carbon. For organic matter in most modern soils, ^{14}C ages higher than 5000 yr before present (BP) are very uncommon (Becker-Heidmann *et al.*, 1988).

^{14}C analysis for the Ap horizon of the non-contaminated site revealed an age of about 1630 yr BP (Table 3) which is an expected value taking into account the permanent dilution of the ^{14}C in the topsoil with modern plant-derived carbon. In contrast, the Ap1 horizon of the contaminated site shows an unusually high ^{14}C age of 15,750 yr BP. The subsoil of the same site was dated as 3840 yr BP. However the non-disturbed subsoil is more than 10,000 yr younger than its topsoil. This pattern is very unusual for natural soils. This is therefore another indication that the topsoil must have been contaminated. Taking into account both the high amounts of organic carbon in the contaminated soil and the very high apparent age of Tertiary brown coal, we conclude that brown coal itself or brown coal-derived products contributed greatly to the measured ^{14}C age.

Due to its Tertiary age brown coal-derived carbon consists only of dead carbon, i.e. carbon free of ^{14}C . Assuming both Ap horizons originally had the same ^{14}C age, we can estimate the degree of contamination with dead carbon by the following equation (Becker-Heidmann, 1989):

$$t_r = -1/\lambda \ln(1 - x)e^{-\lambda t} \quad (3)$$

where: t_r = resulting ^{14}C age; λ = decay rate of ^{14}C ; t = true ^{14}C age; x = relative mass of C contamination (dead carbon).

Taking the determined ^{14}C age of the non-contaminated Ap horizon as t (true ^{14}C age), the mass of the contaminating or anthropogenic C (x) can be calculated as 82% of the total OC. A similar value for the contribution of the contamination (80%) is found calculating the contents of anthropogenic OC as the difference between the contaminated and the non-contaminated soil in Table 2.

The isotopic $\delta^{13}\text{C}$ carbon values for both sites vary around -25‰ relative to the Pee Dee Belemnite (PDB) standard (Table 3). These are common values both for soil humus and C3 plants as well as

Table 3. Radiocarbon ages and $\delta^{13}\text{C}$ values for the Mollisols. ^{14}C dating is reported in years before present (BP)

Sample	^{14}C (a BP)	$\delta^{13}\text{C}$ (‰ PDB)
Ap	Non-contaminated	
	1630 \pm 50	-25.5
Ap 1 BvCv	Contaminated	
	15,750 \pm 170 3840 \pm 60	-25.6 -24.8

for coals (Stout *et al.*, 1981). Therefore, the isotopic $\delta^{13}\text{C}$ values do not give further information about the origin of the organic matter.

Py-GC-MS of bulk samples

The Py-GC-MS traces of the samples are shown as total ion chromatograms (TIC) in Fig. 2. The identified compounds are listed in Table 4. Although several attempts were made, no pyrogram could be obtained for some samples of the non-contaminated site. Presumably due to the low content of organic C (about less than 20 g C/kg), signal intensities in the pyrograms of the bulk soil and the coarser fractions (coarse silt to coarse sand) were too low to allow identification.

The chromatogram of the bulk soil (Fig. 2a) from the contaminated site is dominated by a homologous series of *n*-alkane, *n*-alk-1-ene and α , ω -alkadiene triplets ranging from C_{11} to C_{30} . Prist-1-ene (29) and prist-2-ene (30) are the most abundant components with minor contributions of 4-vinyl guaiacol (20), phenols (10 and 14) and cresol (11 and 12). The chromatogram of the brown coal shows a similar pattern compared with the contaminated sample, with the predominance of prist-1-ene (29) and a homologous series of *n*-alkanes, *n*-alk-1-enes and α , ω -alkadienes, and a minor abundance

of phenol and cresol. In addition, we find benzene (2 and 7), toluene (3), xylene (4 and 5) and trimethyl-benzene (7). A homologous series of *n*-alkanes, *n*-alk-1-enes and α , ω -alkadienes ranging from C_{10} to C_{30} and the pristenes, typical pyrolysis products of kerogen, oil and coal (Philp, 1985; Bracewell *et al.*, 1989) would be expected to be identified in brown coal but not as dominant components in soils (Bracewell *et al.*, 1989). The only reasonable explanation is the contamination of the natural soil by brown coal. A contamination becomes even more evident when particle-size fractions are compared with the brown coal sample.

Py-GC-MS of particle-size fractions

The pyrograms of the size fractions from the non-contaminated site (Fig. 2c-e) show a homologous series of mainly *n*-alkanes. Alkenes are present only as traces with a complete absence of α , ω -alkadienes. The silt fractions show an increased concentration of *n*-alkanes with higher carbon number ($> \text{C}_{22}$) and a carbon number maximum at $n\text{-C}_{25}$. On the other hand, the *n*-alkane in the clay fraction present similar abundance but with a slight predominance at $n\text{-C}_{17}$. Prist-1-ene is present only as trace in all fractions.

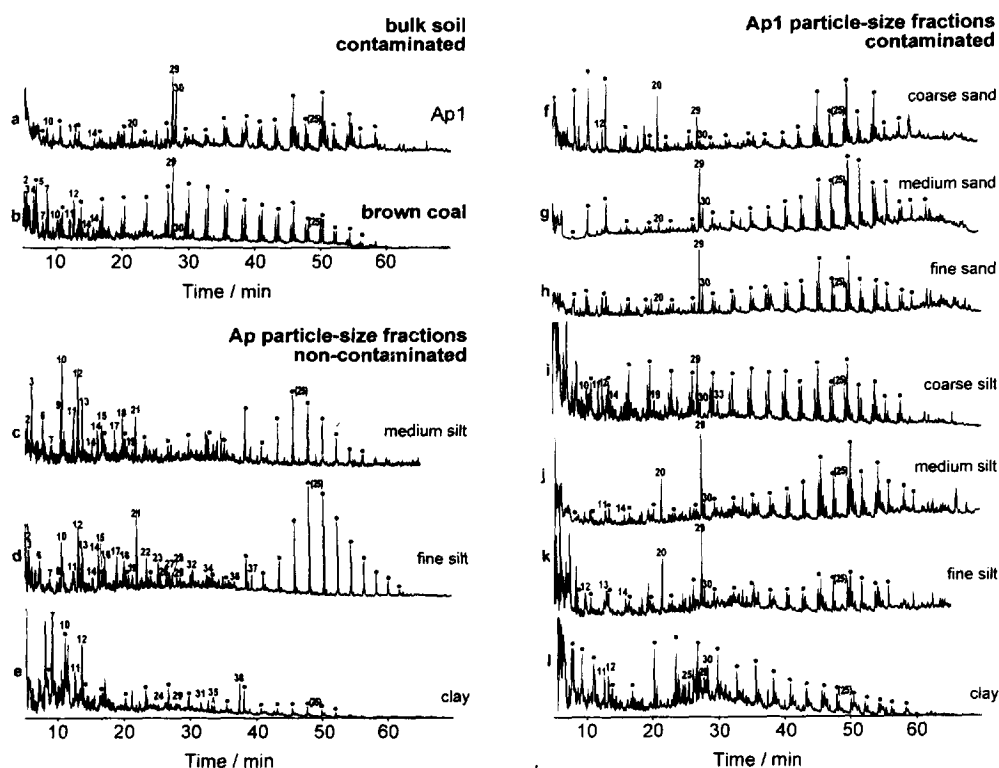


Fig. 2. Total ion chromatogram (TIC) of Py-GC-MS of brown coal, a bulk horizon and particle-size fractions. The particle-size fractions are clay ($< 2 \mu\text{m}$), fine silt ($2\text{--}6 \mu\text{m}$), medium silt ($6\text{--}20 \mu\text{m}$), coarse silt ($20\text{--}63 \mu\text{m}$), fine sand ($63\text{--}200 \mu\text{m}$), medium sand ($200\text{--}630 \mu\text{m}$) and coarse sand ($630\text{--}2000 \mu\text{m}$). The *n*-alkane/*n*-alk-1-ene/ α , ω -alkadiene triplets are indicated as black dots. For display purposes only the $n\text{-C}_{25}$ triplet is marked.

Table 4. Major compounds identified by Py-GC-MS for the contaminated and the non-contaminated site compared with the fractions: (a) Ap1 horizon bulk soil contaminated, (b) brown coal. The fractions are for the non-contaminated soil: (c) medium silt, (d) fine silt, (e) clay; for the contaminated soil: (f) coarse sand, (g) medium sand, (h) fine sand, (i) coarse silt, (j) medium silt, (k) fine silt, (l) clay

#	Compound	Non-contaminated			Brown coal	Contaminated							
		c	d	e	b	a	f	g	h	i	j	k	l
1	3-methylfuran		x										
2	benzene	x	x		x								
3	toluene	x	x		x								
4	<i>o</i> -xylene				x								
5	<i>m/p</i> -xylene				x								
6	dimethylfuran	x	x										
7	C ₃ -benzene	x	x	x	x								
8	5-methylfuran-carboxaldehyde		x										
9	C ₃ -furan	x											
10	phenol	x	x	x	x	x				x			
11	<i>o</i> -cresol	x	x	x	x	x				x	x		x
12	<i>m/p</i> -cresol	x	x	x	x		x			x	x		x
13	guaiacol	x	x									x	
14	C ₂ -phenol	x	x		x	x				x	x	x	
15	methylguaiacol	x	x										
16	methylbenzotriole		x										
17	dihydrobenzofuran	x	x										
18	ethylguaiacol	x	x										
19	methylnaphthalene	x	x							x			
20	4-vinylguaiacol					x	x	x	x		x	x	
21	vinylguaiacol	x	x										
22	indole		x										
23	syringol		x										
24	C ₁₂ -alkylnitrile			x									
25	dimethylnaphthalene												x
26	methylindolycine		x										
27	4-methylsyringol		x										
28	vanillin		x										
29	prist-1-ene		x	x	x	x	x	x	x	x	x	x	x
30	prist-2-ene				x	x	x	x	x	x	x	x	x
31	C ₁₃ <i>n</i> -alkylnitrile			x									
32	acetoguaiacone		x										
33	C ₃ -naphthalene									x			
34	vinylsyringol		x										
35	C ₁₃ -alkylnitrile			x									
36	allylsyringol		x										
37	acetosyringone		x										

Many of the identified aromatic compounds in the non-contaminated sample are related with syringyl and guaiacyl monomers, which are regarded as pyrolysis products of lignin (Saiz-Jimenez and de Leeuw, 1984, 1986; Saiz-Jimenez *et al.*, 1987; Hatcher *et al.*, 1989). For instance, in the silt fractions (Fig. 2c, d) the guaiacyl-based phenols are guaiacol (13), ethylguaiacol (18) and vinylguaiacol (21). The syringyl phenols are syringol (23), 4-methyl syringol (27) and vinylsyringol (34). Other evidence of the pyrolysis of lignin is the presence in all three samples of simple phenols (10 and 14) and cresols (11 and 12) (Saiz-Jimenez and de Leeuw, 1984; Hatcher *et al.*, 1989). Furan-type compounds typically derived from carbohydrates are found in the silt fractions as dimethylfuran (6), 5-methylfuran-carboxaldehyde (8), C₃-furan (9) and dihydrobenzofuran (17) (Bracewell *et al.*, 1989; Zhang *et al.*, 1993). As feature in the clay fraction C₁₂, C₁₃ and C₁₄ alkylnitriles (24, 31 and 38) could be identified. Derenne *et al.* (1992) suggested that nitrogen-containing moieties in algaenan (e.g. from *Chlorella fusca*) are the source of alkylnitriles in pyrolysis products. Finally, although the ¹³C CPMAS spec-

trum of the clay fraction indicates significant intensities in the carbohydrate region between 45 and 110 ppm, no furan-type pyrolysis products could be detected in this fraction by this technique.

Compared to the non-contaminated site, the pyrograms of the particle-size fractions of the contaminated site show a completely different pattern for both aliphatic and aromatic compounds (Fig. 2f-l) and are more similar to the brown coal sample (Fig. 2b). A homologous series of aliphatic compounds ranging from C₁₀ to C₃₀ is characterized by predominance of *n*-alkanes and *n*-alkenes and minor contributions of α , ω -alkadienes. This distribution contrasts with the homologous series of *n*-alkanes in the non-contaminated soil. All the spectra show a distribution of *n*-alkane with carbon number a maximum at C₁₆ for clay and at C₂₄, C₂₆, and C₂₇ for all the other fractions. Except for the clay and the coarse sand fraction, prist-1-ene is the most intense peak in the pyrograms.

Aromatic compounds, especially those associated with lignin or altered lignin, are less abundant in the pyrolyzates of the contaminated soil compared to the corresponding fractions from the non-con-

taminated site. For example, the lignin derived syringyl and guaiacyl units can hardly be detected in the contaminated soil. In the clay fraction only phenol, cresol and dimethylnaphthalene are identified, similar to the clay of the non-contaminated soil. Simple phenols and cresols are typical pyrolysis products obtained from soils as well as from coal (Bracewell *et al.*, 1989). Fine and medium silt are

characterized by the presence of guaiacol (13), 4-ethylguaiacol (18) and 4-vinylguaiacol (20), which are possibly lignin-derived compounds. Compared to the corresponding non-contaminated fractions, the abundance of lignin-derived components is notably low. The same is true for the sand fractions, where 4-vinylguaiacol (20) and 4-methylsyringol (27) are the only lignin-derived compounds.

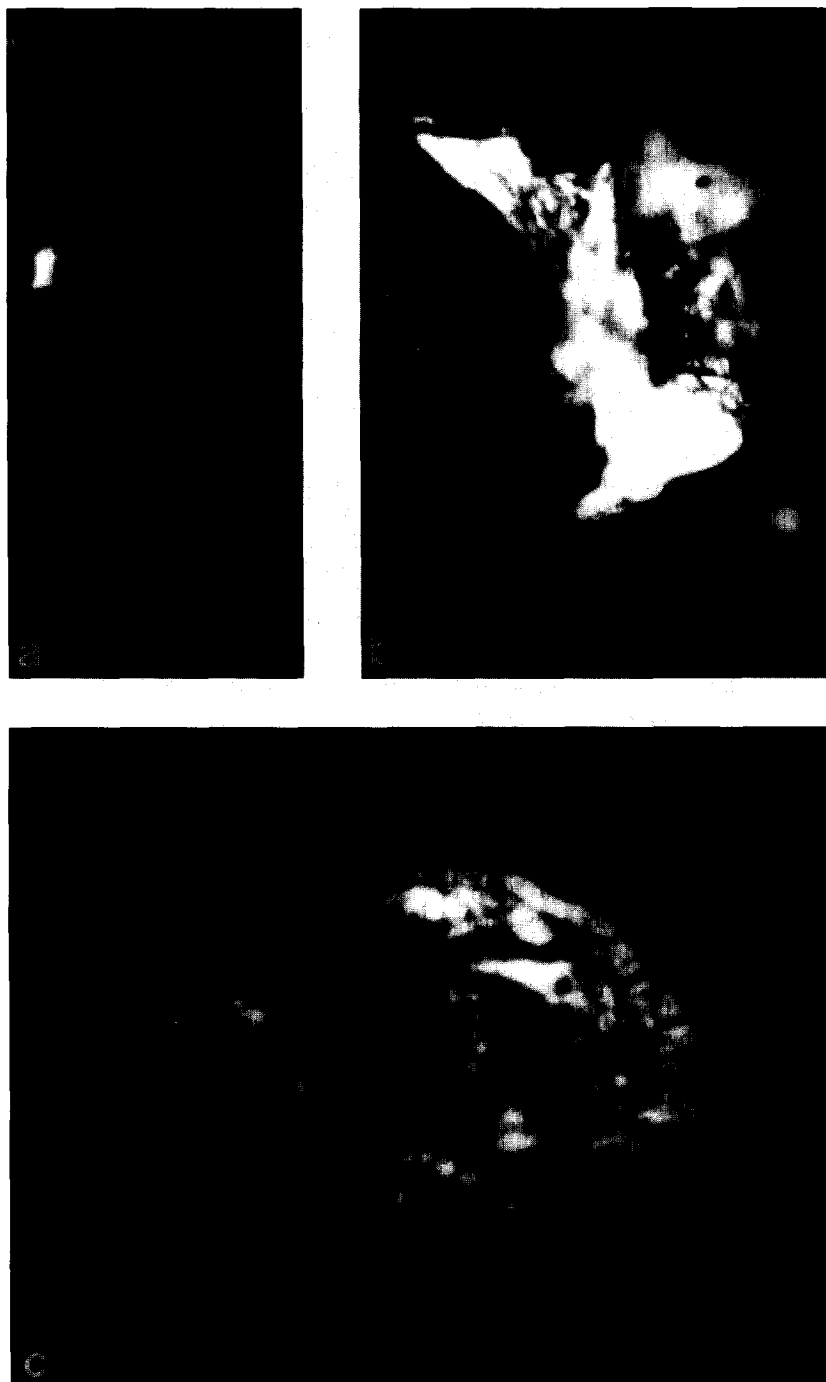


Fig. 3. Photomicrographs of the fine sand (63–200 μm) fraction of the contaminated Ap1 horizon: (a) sporonite particle (length 13 μm), (b) coke particle (length 40 μm) and (c) coke particle with a rim of graphite condensed from the gas phase (length 45 μm).

The Py-GC-MS investigations reveal significant differences between the respective samples from the non-contaminated and the contaminated site. The chromatograms of the non-contaminated particle-size fractions show a homologous series of mainly *n*-alkanes with *n*-alkenes present only at trace levels, and with a lack of α , ω -alkadienes. Prist-1-ene is detected only as a trace in the fractions of the non-contaminated soil. Mainly lignin- and carbohydrate-derived units are found in the silt fractions and alkylnitriles in the clay fraction, whereas, the contaminated soil is more similar to the brown coal, with the same homologous series of *n*-alkanes, *n*-alkenes, α , ω -alkadienes and a predominance of prist-1-ene (except for the clay fraction). Lignin- and carbohydrate-derived compounds are less abundant. The Py-GC-MS data suggest that the contaminated soil and the corresponding size fractions are heavily influenced by the brown coal compared to the non-contaminated soil. Again, the data show that the clay fraction of the contaminated soil contains less brown coal-derived components compared to the medium and coarse particle-size classes.

Reflected light microscopy

The fine sand fraction of the contaminated soil, rich in organic C, offered the best evidence of the presence of contaminant particles. Due to the optical properties of the immersion oil, quartz grains are not visible. The majority of the visible particles (about 90% of the area) are organic materials. Brown coal with its major component maceral groups (huminite, liptinite and inertinite) dominates this organic fraction. Because brown coal typically displays a low optical contrast in reflected light microscopy no suitable photos of these particles could be taken. The low reflectance of the huminite, liptinite and sporonite particles (Fig. 3a) indicates that this brown coal has not undergone any significant thermal alteration. Nevertheless, some (10–20%) of the visible organic particles are thermally altered brown coal, coke particles (Fig. 3b) or coke particles with a rim of graphite which was formed probably by condensation from the gas phase (Fig. 3c), a characteristic byproduct of industrial heating or combustion (Chandra and Taylor, 1982). About 10% of the visible particles are mineral matter. Some of these particles can be identified as iron sulfides or iron oxides. Finally, the microscopic study confirms the hypothesis that the majority of the organic substances in the contaminated soil is from brown coal dust. Only minor amounts of thermally degraded brown coal or coke particles are identified.

CONCLUSIONS

By a combination of bulk methods (elemental analysis, reflectance microscopy), ^{14}C dating and

modern spectroscopic techniques (^{13}C CPMAS-NMR, Py-GC-MS) the contamination of a soil from Halle (East Germany) could be characterized as being mainly brown coal dust and small amounts of coke particles. Consequently, the organic matter in the contaminated soil is a mixture of native soil-derived humic substances and brown coal dust and coke particles.

The quantitative impact of the brown coal dust emissions on the soil of the contaminated site results in a significant increase of C and N contents in the bulk soil, by a factor of six for C and a factor of two for N. Significant amounts of the C found in the contaminated soil are of anthropogenic origin (80–82%). In the size fractions C and N contents are variable, but are highest for medium silt to fine sand fractions. The calculated amount of anthropogenic C decreases from the coarse sand to the clay fraction suggesting that the emissions of the brown coal dust affected mainly the coarse particle-size fractions.

CPMAS ^{13}C NMR reveals that the organic matter of the contaminated soil is characterized by higher relative amounts of aliphatic carbon compared to the non-contaminated site. The relative amount of aromatic carbon as determined by CPMAS ^{13}C NMR is similar in both the contaminated and the non-contaminated soil. However, the molecular composition of the aromatic carbon as obtained from the Py-GC-MS fraction is different. Pyrolysis products derived from (degraded) lignin are more abundant in the non-contaminated soil, simple phenols and cresols predominate in the contaminated soil. Both methods indicate that the structural chemical alterations due to the input of brown coal are more pronounced in the silt and sand fractions than in the clay fraction. This is in accordance with the finding that the clay fraction contains higher relative amounts (about 50%) of native soil organic matter.

Acknowledgements—This work was financially supported by the Deutsche Forschungsgemeinschaft (Ko 1035/6-1) and the Deutscher Akademischer Austauschdienst (Ref. 315, D/94/16993). For help during site selection we would like to thank Dr. W. Heisig (University of Halle) and Dr. C. Moritz (Merseburg). Experimental assistance was provided by W. Gosda and G. Wilde (University of Bochum). ^{14}C dating was performed by Dr. P. Becker-Heidmann (University of Hamburg). We thank Dr A. Davis (Pennsylvania State University) for his assistance in obtaining reflected light microscopic information. The critical comments of an anonymous reviewer are gratefully acknowledged.

REFERENCES

- AG Bodenkunde (1994) *Bodenkundliche Kartieranleitung*. Schweizerbart'sche Verlagsbuchhandlung, 4th Ed., Hannover, Germany.

- Baldock J. A., Oades J. M., Waters A. G., Peng X. and Vasallo A. M., Wilson M. A. (1992) Aspects of the chemical structure of soil organic materials as revealed by solid-state ^{13}C NMR spectroscopy. *Biogeochemistry* **16**, 1–42.
- Becker-Heidmann P. (1989) Die Tiefenentwicklung der natürlichen Kohlenstoff-Isotopengehalte von vollständig dünn-schichtweise beprobten Parabraunerden und ihre Relation zur Dynamik der organischen Substanz in diesen Böden. Ph. D. Thesis, Hamburger Bodenkundliche Arbeiten 13, University of Hamburg.
- Becker-Heidmann P., Liang-wu L. and Scharpenseel H. W. (1988) Radiocarbon dating of organic matter fractions of a Chinese Mollisol. *Z. Pflanzenernähr. Boden.* **151**, 37–39.
- Bracewell J. M., Haider K., Larter S. R. and Schulten H.-R. (1989) Thermal degradation relevant to structural studies of humic substances. In *Humic Substances II* (Edited by Hayes M. H. B., MacCarthy P. and Swift R. S.), pp. 181–222. Wiley, New York.
- Chandra D. and Taylor G. H. (1982) Thermally altered coals. In *Stach's Textbook of Coal Petrology* (Edited by Stach E., Mackowsky M.-T., Teichmüller M., Taylor G. H., Chandra D. and Teichmüller R.), pp. 206–218. Borntraeger, Berlin.
- Christensen B. T. (1985) Carbon and nitrogen in particle-size fractions isolated from Danish arable soils by ultrasonic dispersion and gravity-sedimentation. *Acta Agric. Scand.* **35**, 175–187.
- Christensen B. T. (1992) Physical fractionation of soil and organic matter in primary particle-size and density separates. In *Advances in Soil Science* 20 (Edited by Stewart B. A.), pp. 1–90. Springer, New York.
- Dalal R. C. and Bridge B. J. (1996) Aggregation and organic matter storage in sub-humid and semi-arid soils. In *Structure and Organic Matter Storage in Agricultural Soils* (Edited by Carter M. A. and Stewart B. A.), pp. 263–307. *Advances in Soil Science*, Springer, New York.
- Depers A. M. and Yassini I. (1994) Petrography of natural and industrial particulate materials deposited into Lake Illawara, New South Wales, Australia. In *46th Annual Meeting of the International Committee for Coal and Organic Petrology, Commissions I/II/III, Working Group on Environmental Applications of Coal Petrology* (Edited by Depers A. M. and Bailey J. G.), pp. 20–21.
- Derenne S., Largeau C. and Hatcher P. G. (1992) Structure of *Chlorella fusca* algaenan: relationships with ultralaminae in lacustrine kerogens; species- and environment-dependent variations in the composition of fossil ultralaminae. *Org. Geochem.* **18**, 417–422.
- Fredericks P. M., Warbrook P. and Wilson M. A. (1983) Chemical changes during natural oxidation of a high volatile bituminous coal. *Org. Geochem.* **5**, 89–97.
- Garbarini D. R. and Lion L. W. (1986) Influence of soil organics on the sorption of toluene and trichloroethylene. *Environ. Sci. Technol.* **20**, 1263–1269.
- Grathwohl P. (1990) Influence of organic matter from soils and sediments from various origins on the sorption of chlorinated aliphatic hydrocarbons: implications on K_{oc} correlations. *Environ. Sci. Technol.* **24**, 1687–1693.
- Guggenberger G., Zech W., Haumaier L. and Christensen B. T. (1995) Land use effects on the composition of organic matter in particle-size separates in soils: II. CPMAS and solution ^{13}C NMR analysis. *Eur. J. Soil Sci.* **46**, 147–158.
- Hatcher P. G., Wilson M. A., Vasallo A. M. and Lerch H. E. (1989) Studies of angiospermous woods in Australian brown coals by nuclear magnetic resonance and analytical pyrolysis: new insights into early coalification. *Int. J. Coal Geol.* **13**, 99–126.
- Kopinke F.-D., Pörschmann J. and Stottmeister U. (1995) Sorption of organic pollutants on anthropogenic humic matter. *Environ. Sci. Technol.* **29**, 941–950.
- Meiler W. and Meusinger R. (1991) NMR of coals and coal products. *Annual Reports on NMR Spectroscopy* **23**, 375–410.
- Neumeister H., Franke C., Nagel C., Peklo G., Zierath R. and Peklo P. (1991) Immissionsbedingte Stoffeinträge aus der Luft als geomorphologischer Faktor. 100 Jahre atmosphärische Deposition im Raum Bitterfeld (Sachsen-Anhalt). *Geoökodynamik* **12**, 1–40.
- North P. F. (1976) Towards an absolute measurement of soil structural stability using ultrasound. *J. Soil Sci.* **27**, 451–459.
- Philp R. P. (1985) *Fossil Fuel Biomarkers*. Elsevier, Amsterdam.
- Pisupati S. V., Scaroni A. W. and Hatcher P. G. (1993) Devolatilization behaviour of naturally weathered and laboratory oxidized bituminous coals. *Fuel* **72**, 165–173.
- Saiz-Jimenez C. and de Leeuw J. W. (1984) Pyrolysis-gas chromatography mass spectrometry of isolated, synthetic and degraded lignins. *Org. Geochem.* **6**, 417–422.
- Saiz-Jimenez C. and de Leeuw J. W. (1986) Lignin pyrolysis products: their structures and their significance as biomarkers. *Org. Geochem.* **10**, 869–876.
- Saiz-Jimenez C., Boon J. J., Hedges J. J., Hessels J. K. C. and de Leeuw J. W. (1987) Chemical characterization of recent and buried woods by analytical pyrolysis. Comparison of pyrolysis data with ^{13}C NMR and wet chemical data. *J. Anal. Appl. Pyrol.* **11**, 437–450.
- Schmidt M. W. I. and Kögel-Knabner I. (1995) Bedeutung der Struktur organischer Sorbenten für die Bindung Hydrophober organischer Umweltchemikalien. *Z. Geol. Wiss.* **23**, 211–218.
- Shneur E. (1966) Oxidation of graphite carbon in certain soils. *Science* **155**, 991–992.
- Simonson R. W. (1995) Airborne dust and its significance to soils. *Geoderma* **65**, 1–43.
- Skjemstad J. O., Clarke P., Taylor J. A., Oades J. M. and Newman R. H. (1994) The removal of magnetic materials from surface soils. A solid state ^{13}C CP/MAS n.m.r. study. *Aust. J. Soil Res.* **32**, 1215–1229.
- Soil Survey Staff (1994) *Keys to Soil Taxonomy*. U.S. Department of Agriculture, Pocahontas Press, Virginia.
- Stout J. D., Goh K. M. and Rafter T. A. (1981) Chemistry and turnover of naturally occurring resistant organic compounds in soil. In *Soil Biochemistry V* (Edited by Paul E. A. and Ladd J. N.), pp. 1–73. Dekker, New York.
- Stuiver M. and Polach H. (1977) Discussion: reporting of ^{14}C data. *Radiocarbon* **19**, 355–363.
- Wik M. and Renberg I. (1987) Distribution in forest soils of carbonaceous particles from fossil fuel combustion. *Water Air Soil Pollut.* **33**, 125–129.
- Wilson M. A. (1987) *NMR Techniques and Applications in Geochemistry and Soil Chemistry*. Pergamon Press, Oxford.
- Zhang E., Hatcher P. G. and Davis A. (1993) Chemical composition of pseudo-phlobanite precursors: implications for the presence of aliphatic biopolymers in vitrinite from coal. *Org. Geochem.* **20**, 721–734.